The Dianion of [18]Annulene[1]

J. F. M. Oth,* E. P. Woo, and F. Sondheimer

Contribution from the Laboratory for Organic Chemistry, Swiss Federal Institute of Technology, 8006 Zürich, Switzerland, and University College, London WC1H OAJ, England. *Received May 2, 1973*

Abstract: The dianion of [18]annulene has been prepared by reduction of [18]annulene in THF-d_8 with potassium. The ^{1}H-nmr spectrum at $-110°$ clearly indicates that the dianion exists in solution as an equilibrium between two species (relative amounts: 70 and 30%). These two species are believed to be two conformers of the [18]-219-annulene dianion, to exhibit π-bond localization, and to be nonplanar. Both species have six intraannular and 12 extraannular protons. They sustain a paramagnetic ring current: the signal of the inner protons appears at τ −19.5 and −18.1, while that of the outer protons appears at τ 11.13 (at $-110°$). Increase in temperature brings about the nmr equivalence of all protons. This can be understood if a fast interconversion of the two conformers, together with a fast π-bond shift process in each one, takes place. From the activation free energy estimated for the bond-shift process it can be deduced that the resonance energy associated with a 20-electron π-bond system delocalized over 18 carbon atoms is negative and of the order of −5 to −8.7 kcal mol.$^{-1}$

[18]Annulene (**1**)[2] conforms approximately to the D_{6h} symmetry group;[3,4] no bond alternation (in the sense of successive "single" and "double" bonds) exists in this molecule. The π-bond delocalization is also clearly demonstrated by the positions of the signals of the two types of protons (inner and outer protons) in the ^{1}H-nmr spectrum at low temperature; they indicate that the [18]annulene molecule sustains[5,6] a diamagnetic ring current.[7]

The [18]annulene molecule was also shown[6] to undergo an isodynamic[8] conformational mobility by which each proton can occupy either of the two magnetic sites characteristic of the molecule. A mechanism has been proposed[6] for this process which implies that *three* isodynamic structures of type **1**[9] are in dynamic equilibrium and that structures of type **2**[9] (six) are probable intermediates along the interconversion pathway.

We have investigated how the nature of the π bonding (π-bond alternation or π-bond delocalization) might be modified by reducing the [18]annulene to its dianion. The following theoretical points are of particular interest.

(i) The dianion of [18]annulene, possessing 20 π electrons (a $4n$ π system) may be expected to exhibit π-bond alternation, since the resonance energy associated with 20 π electrons on a delocalized π-bond system is calculated by the SCF–MO method to be negative.[11] The occurrence of π-bond alternation would reduce the symmetry of the dianion (to D_{3h}, D_3 symmetry, or below) relative to that of the neutral molecule (D_{6h}).

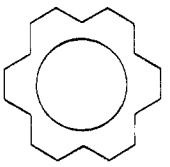

1
[18]-219-annulene conformation of D_{6h} symmetry

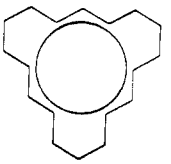

2
[18]-219-annulene conformation of D_3 or C_2 symmetry

(ii) What is the exact symmetry of the dianion in its electronic ground state? In a geometry with a C_3 axis, the two lowest antibonding MO's would be degenerate and the ground state could be either a singlet or a triplet. As shown below, the normal nmr spectrum observed for the dianion indicates that the ground state is a singlet. Its symmetry species can be either A or E. If, due to configuration interaction, the latter (E) corresponds to a lower energy, one would expect that the C_3 axis be removed by a weak Jahn–Teller distortion.[12] Hence, there is a definite possibility that the symmetry of the dianion will be further reduced below that already induced by π-bond localization.

(iii) If the dianion shows π-bond localization, it must also exhibit a conformational mobility (which must be much faster than that observed in the neutral molecule) and possibly an isodynamical bond-shift process, such as the one observed in the neutral [$4n$]-annulenes[10] (*i.e.*, in [8]-[13] and [16]annulene[14]). Con-

(1) This paper is part LXXXIX in the series on Unsaturated Macrocyclic Compounds. For part LXXXVIII, see K. Stöckel and F. Sondheimer, *J. Chem. Soc., Perkin Trans. 1*, 355 (1972).

(2) F. Sondheimer, R. Wolovsky, and Y. Amiel, *J. Amer. Chem. Soc.*, 84, 274 (1962).

(3) J. Bregman, F. L. Hirschfeld, D. Rabinovich, and G. M. J. Schmidt, *Acta Crystallogr.*, 19, 227 (1965).

(4) F. L. Hirschfeld and D. Rabinovich, *ibid.*, 19, 235 (1965).

(5) F. Sondheimer, *Proc. Roy. Soc., Ser. A*, 297, 173 (1967); F. Sondheimer, J. A. Elix, Y. Gaoni, P. J. Garratt, K. Grohmann, G. di Maio, J. Mayer, M. V. Sargent, and R. Wolovsky, *Chem. Soc., Spec. Publ.*, No. 21, 75 (1967), and references cited there.

(6) J.-M. Gilles, J. F. M. Oth, F. Sondheimer, and E. P. Woo, *J. Chem. Soc. B*, 2177 (1971).

(7) See J. A. Pople, W. G. Schneider, and H. J. Bernstein, "High-Resolution Nuclear Magnetic Resonance," McGraw-Hill, New York, N. Y., 1959, and references cited there.

(8) S. L. Altmann, *Proc. Roy. Soc., Ser. A*, 298, 184 (1967). An isodynamic transformation, by definition, leaves the electronic Hamiltonian invariant. It effects a reorientation of the nuclear skeleton and a redistribution of nuclei among the sites of this skeleton.

(9) Structures 1 and 2 may be regarded as two conformers having the same configuration if the configuration is characterized by the stereochemical nature (cis or trans) and the sequence of the double bonds in the Kekulé structures. Both 1 and 2 have thus the following sequence of double bonds: cis, trans, trans, cis, trans, trans, cis, trans, trans (*i.e.*, the configuration 219 in our coded notation given in ref 10).

(10) J. F. M. Oth, *Pure Appl. Chem.*, 24, 573 (1971).

(11) M. J. S. Dewar and G. J. Gleicher, *J. Amer. Chem. Soc.*, 87, 685 (1965).

(12) In the case of a species with two degenerate MO's containing two electrons, the only effective contributions to a Jahn–Teller effect must originate in two-electron terms in the Hamiltonian. See, for instance, M. H. Perrin, M. Gouterman, and Ch. L. Perrin, *J. Chem. Phys.*, 50, 4137 (1969).

(13) F. A. L. Anet, *J. Amer. Chem. Soc.*, 84, 671 (1962); F. A. L. Anet, A. J. R. Bourn, and Y. S. Lin, *ibid.*, 86, 3576 (1964).

(14) G. Schröder and J. F. M. Oth, *Tetrahedron Lett.*, 4083 (1966); J. F. M. Oth and J.-M. Gilles, *ibid.*, 6259 (1968).

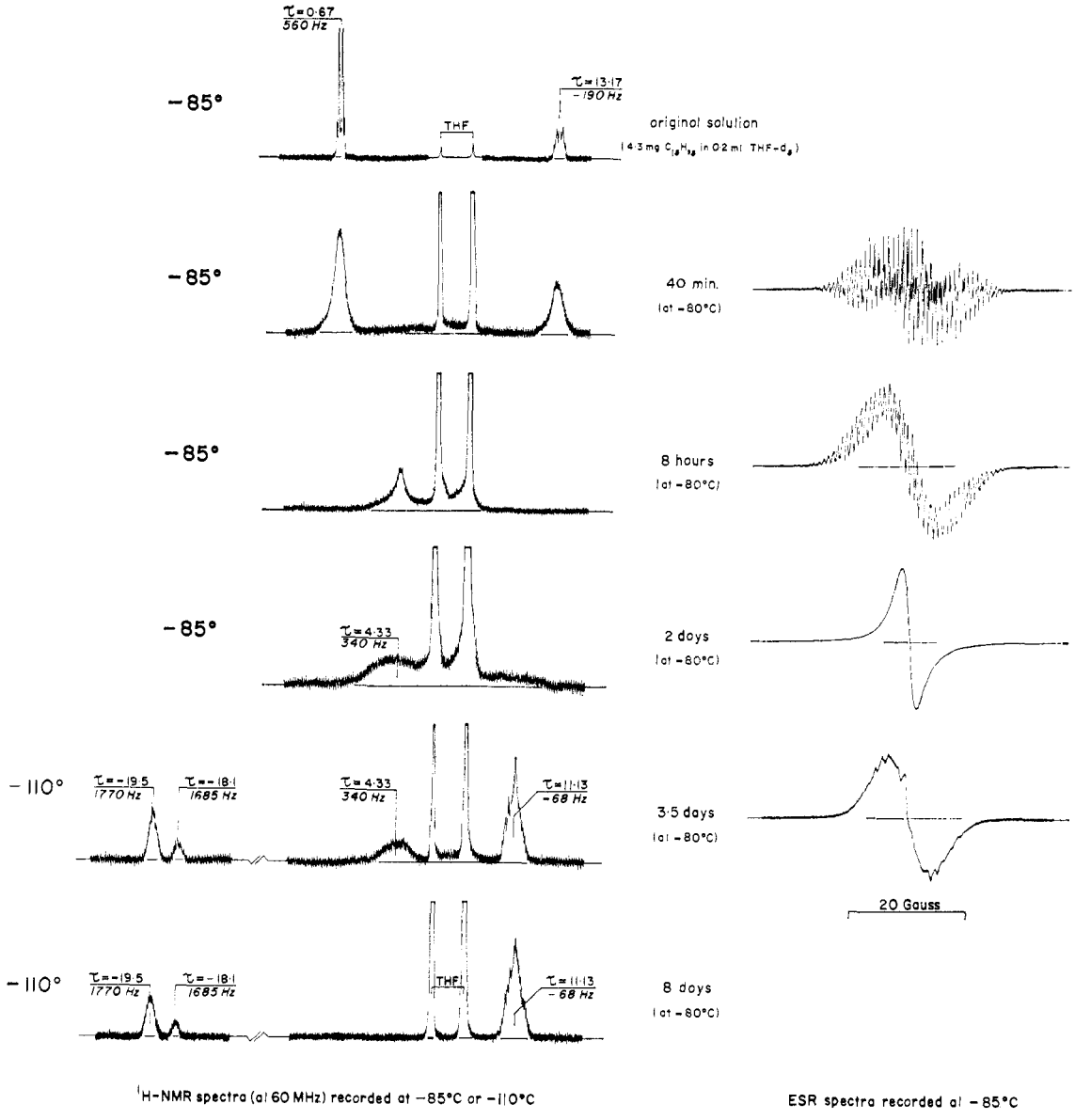

Figure 1. The reduction of [18]annulene into its dianion by potassium. The 60-MHz ^{1}H-nmr (at -85 or $-110°$) and esr (at $-85°$) spectra obtained after various contact times between the solution of [18]annulene and potassium.

sequently the ^{1}H-nmr spectrum of the [18]annulene dianion may be expected to be temperature dependent.

We report here on the preparation of the dianion of [18]annulene, on the elucidation of its structure (based on its ^{1}H-nmr spectrum), and on the dynamic behavior of this nonaromatic species.

Experimental Section

A. Polarography of [18]Annulene. The possibility of the reduction of [18]annulene to its dianion was first studied by classical and by oscilloscopic (cyclic voltametry) polarography.[15] Two reversible reduction waves corresponding to the reduction of [18]-annulene into the radical anion $R\cdot$ and of the radical anion into the dianion R^{2-} were observed (in dimethylformamide with tetra-*n*-butylammonium perchlorate as supporting electrolyte). Their half-wave potentials are given in Table I. These results indicate that the dianion of [18]annulene can be prepared by reduction with alkali metals.

B. Preparation and ^{1}H-nmr Spectrum of the [18]Annulene Dianion. The dianion of [18]annulene could only be prepared under scrupulously dry conditions by reacting a dilute solution of the annulene in THF-d_8 with potassium at $-80°$ and maintaining this temperature until the reduction was complete. The potassium was extruded into the upper part of an adequately constricted nmr tube containing [18]annulene (4.3 mg). The THF-d_8 (0.2 ml) was then condensed onto the annulene and the tube was sealed. The potassium wire was then partly evaporated and condensed on the glass wall as a bright mirror in the upper end of the tube (an induction furnace was used for this). The ^{1}H-nmr spectrum of the initial solution was recorded at $-85°$ for reference. The solution was then brought into contact several times with the potassium at $-80°$ by inverting the nmr tube. After each period of known contact time the ^{1}H-nmr spectrum (at -85 or $-110°$) and the esr spectrum (at $-85°$) were recorded. Figure 1 shows some of the most characteristic spectra.

The two signals characteristic of the neutral molecule at τ 0.67

Table I

	$E_{1/2}$ (0°),[a] V	Reversibility	ne^-	Process
1st wave	−1.56	rev.	1	$R + 1e^- \rightleftharpoons R\cdot^-$
2nd wave	−1.90	rev.	1	$R\cdot^- + 1e^- \rightleftharpoons R^{2-}$

[a] Potentials with respect to the reference electrode $Hg|Hg_2Cl_2|KCl$ (0.1 *N*, aqueous).

(15) The polarograph used will be described elsewhere: J. F. M. Oth and P. Jung, submitted for publication.

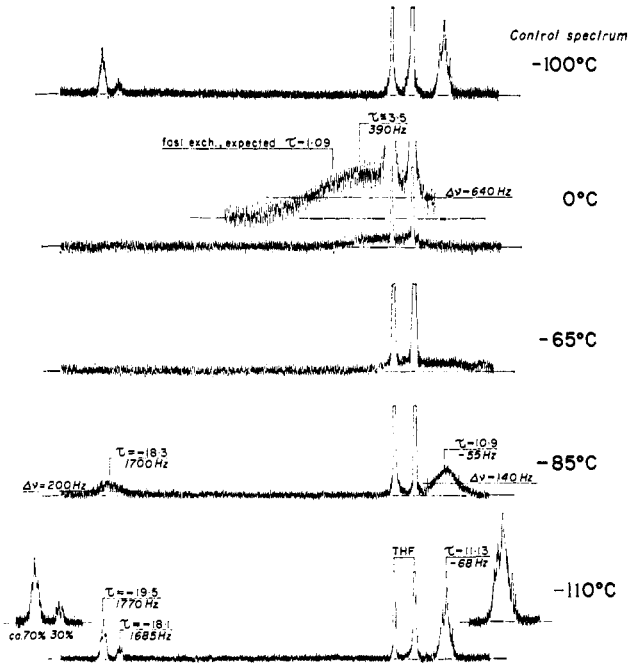

Figure 2. Temperature dependence of the ^{1}H-nmr spectrum (at 60 MHz) of the dianion of [18]annulene (as the potassium salt).

(outer protons) and 13.17 (inner protons) were broadened after several minutes contact time; the solution also showed an esr spectrum with well-resolved fine structure; both observations indicate the appearance of the radical anion. After 8 hr of contact, the two nmr signals of the neutral molecule had disappeared and a new signal at τ 4.33 was observed. After 2 days contact, this new signal[16] appeared as a broad band while the esr signal showed its maximum intensity but no fine structure. Longer contact time between the solution and the metal led to the appearance of three new nmr signals at τ −19.5, −18.1, and 11.13. After longer contact (8 days), only these signals remained and no esr signal was observed. We attribute this last ^{1}H-nmr spectrum to the pure dianion of [18]annulene.

C. Temperature-Dependent ^{1}H-Nmr Spectrum of the [18]Annulene Dianion. At −110°, the high-field signal (τ 11.13) (Figure 2) of the dianion has a relative intensity of 12 while the two low-field signals (τ −19.5, −18.1) have, in total, a relative intensity of 6. The high-field signal being more intense must be attributed to the outer protons and the low-field signal to the inner protons. The intensities of the two low-field signals are in the ratio of 4.2 (τ −19.5) to 1.8 (τ −18.1). This noninteger ratio indicates that two species (each with 12 outer and six inner protons) are present in the relative amounts of 70 and 30%. The unusual chemical shifts of the different protons clearly indicate that these two species sustain a paramagnetic ring current.[17] A poorly resolved triplet structure is detectable in the low-field signals, indicating that in each species all the inner protons have the same chemical shift and are coupled with two vicinal outer protons with an average coupling constant of *ca.* 14 Hz. Some structure is also visible in the signal of the external protons.

The ^{1}H-nmr spectrum of the dianion of [18]annulene is temperature dependent, as can be seen in Figure 2. This temperature dependence is reversible, as indicated by the fact that the −110° spectrum is retained after heating the sample to 0° and subsequent cooling. This also means that the dianion is relatively stable at 0°; however, above 0° the dianion is rapidly destroyed, possibly due to reaction with the solvent.

The two low-field signals due to the inner protons in the two chemical species present coalesce at −85° into a broad signal at τ −18.3, while the signal at high field also broadens. These signals coalesce around −65° and, at 0°, only one broad band (line width, 640 Hz) centered at *ca.* τ 3.5 is observed; all the protons are now magnetically equivalent. (In the very fast exchange limit, the signal is expected to appear at τ 1.09, if one neglects the probable variation of the chemical shifts with temperature.) This temperature dependence of the nmr spectrum indicates that the two species present undergo fast isodynamic processes and fast interconversion.

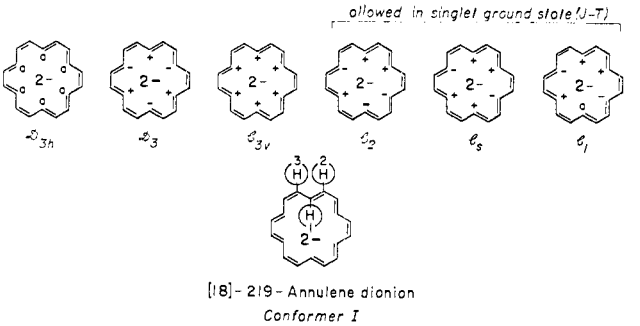

Figure 3. Possible geometries of conformer I of the [18]-219-annulene dianion, assuming π-bond localization.

Discussion

A. Structure of the Dianion of [18]Annulene. The ^{1}H-nmr spectrum observed at −110° and the temperature dependence are best understood if one assumes that the two species in question are the two conformers I and II of the [18]annulene dianion with the 219 configuration (cis, trans, trans, cis, trans, trans, cis, trans, trans).[10] Species I and II are expected to show π-

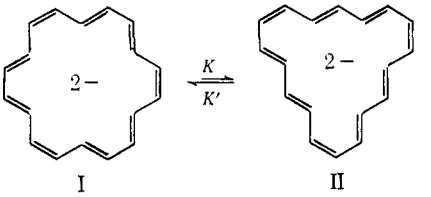

bond localization and are most likely nonplanar, the nonbonding interactions between the inner protons then being relieved.

The possible geometries for the species I and II are shown in Figures 3 and 4, respectively. Among the different geometries considered some have no C_3 symmetry axis. In these geometries of low symmetry the two lowest antibonding MO's are no longer degenerate and a singlet ground state is expected. A minimum of *three* different magnetic sites is expected in conformer I and at least *six* different magnetic sites are expected in conformer II. These sites have been numbered for identification in Figures 3 and 4.

Both conformers I and II have six inner and 12 outer protons. Assuming that the resonance signals of the two types of inner protons in conformer II (on sites 1′ and 3′) appear at the same position,[18] then a 70/30 equilibrium between the two conformers can very well explain the ^{1}H-nmr spectrum observed at −110°. The unusual chemical shifts observed for the different protons of I and II can also be understood as follows. The paramagnetic shifts due to the paramagnetic ring

(16) This signal has to be assigned to neutral molecules undergoing fast electron exchange with the radical anions and/or the dianions present. Note that the esr signal indicates exchange narrowing at this stage of reduction (after 2 days contact).

(17) J. A. Pople and K. G. Untch, *J. Amer. Chem. Soc.*, 88, 4811 (1966).

(18) This is certainly the case at −110°, since, due to fast bond shift, these two sites (1′ and 3′) become equivalent on the nmr time scale (see below in text).

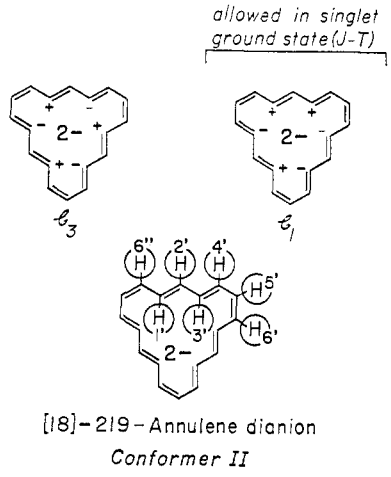

Figure 4. Possible geometries of conformer II of the [18]-219-annulene dianion, assuming π-bond localization.

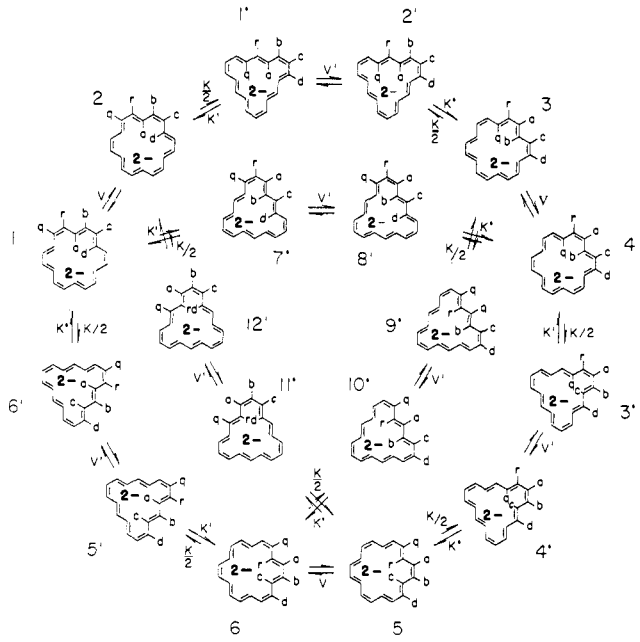

Figure 5. Exchange mechanism postulated to explain the magnetic equivalence of all the protons of the [18]annulene dianion above *ca.* $-65°$ at 60 MHz. Ground-state structures with localized π bonds (I and II, hypothesis 1) are considered.

current induced in a cyclic $4n$ π-electron system were shown theoretically to tend toward an infinite value[17] (toward minus infinity for the inner protons and plus infinity for the outer protons) when all the bond lengths of the ring tend toward equality (π-bond delocalization) and provided that the ring is planar. π-Bond alternation and out of plane deformation are two distortions which quench the paramagnetic ring current and thus reduce the paramagnetic shifts. These distortions, which are supposed to occur in I and II, thus reduce the paramagnetic shifts to the finite values observed. It also seems reasonable to assign the signal at τ -19.5 to the inner protons of the conformer which can more closely approach planarity, *i.e.* conformer I; the signal at τ -18.1 is then assigned to the inner protons of conformer II.

The poorly resolved triplet structure observed in the signals of the inner protons (Figure 2, spectrum at $-110°$) indicates an average coupling constant be-

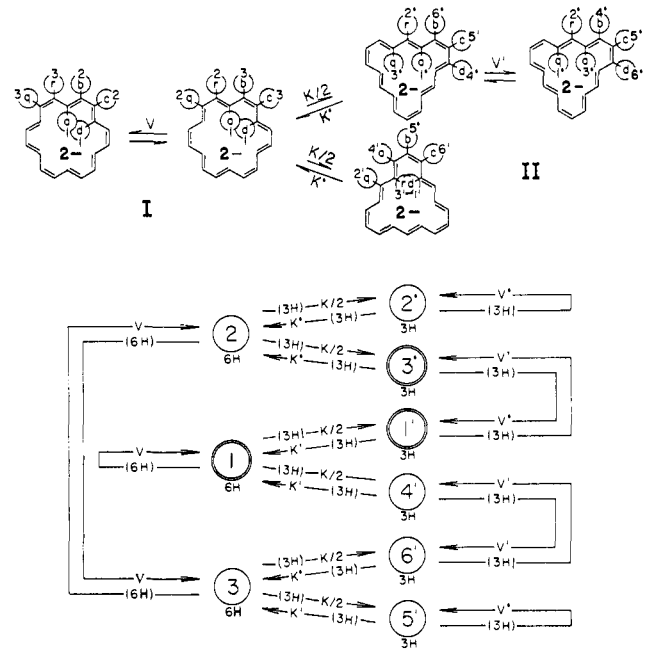

Figure 6. Exchange diagram for the [18]annulene dianion. I and II represent structures with localized π bonds which undergo π-bond shift (V and V') and which interconvert by a conformational process (K and K') (hypothesis 1).

tween each inner proton and the two vicinal outer ones of: in conformer I, $^1/_2[^3J_{12} + {}^3J_{13}] = 14$ Hz; in conformer II, $\tau_{1'} = \tau_{3'} = -18.1$ at $-110°$ and $^1/_2[^3J_{1'2'} + {}^3J_{1'6''}] = {}^1/_2[^3J_{3'2'} + {}^3J_{3'4'}] = 14$ Hz. Average coupling constants as well as apparent identity of $\tau_{1'}$ and $\tau_{3'}$ are due to fast π-bond shift in each conformer. The value $\langle J \rangle = 14$ Hz indeed corresponds well to the mean value of one coupling through a trans double bond and one coupling through a gauche single bond.

The ^{1}H-nmr spectrum observed at $-110°$ favors structures with localized π bonds, the paramagnetic ring current being mostly quenched by π-bond alternation. This π-bond situation is strongly supported by the fast dynamic processes exhibited by the two species I and II.

B. The Dynamic Processes in the Dianion of [18]-219-Annulene. Three situations could explain qualitatively the complete exchange of all the protons on all magnetic sites observed above $-65°$ (see Figure 2).

(1) The two species involved are the two conformers I and II of the [18]-219-annulene dianion discussed above; *i.e.*, they have localized π bonds and are nonplanar. They interconvert into each other very quickly, this process requiring only rotation around single bonds (such a process was observed in the [4*n*] annulenes and requires only a small activation energy).[10] However, this conformational mobility is not sufficient to exchange the protons on all magnetic sites. But if π-bond shift takes place in each conformer, then complete exchange of all the protons on all magnetic sites is expected. Six isodynamic structures I (1–6 in Figure 5) and 12 isodynamic structures II (1′–12′ in Figure 5) are implied in this situation, as is indicated in

Figure 5. The exchange diagram characterizing this situation is shown in Figure 6. From this diagram we can see that conformational mobility (K and K') and π-bond shift (at least in conformer II, *i.e.* V') are indeed required to lead to complete exchange of the protons on all nine different magnetic sites. We also see that π-bond shift in structure II *must* always take place (with K and K') in order to lead to complete exchange, while bond shift in I is not necessarily required (bond shift in I alone combined with K and K' would lead to partial exchange). However, there are no reasons why bond shift would occur in conformer II and not in conformer I.

(2) The temperature dependence of the ^{1}H-nmr spectrum could also be explained if we assume that the two conformers are in dynamic equilibrium with a small amount of neutral molecule (and radical anion) rather than undergoing π-bond shift. (The amount of unreduced [18]annulene has to be smaller than 5%, otherwise it would be detectable in the ^{1}H-nmr spectrum at $-110°$.) Fast reversible electron exchange between the dianion and the neutral [18]annulene would then have the same result as the π-bond shift processes. We can summarize this electron exchange by the equation

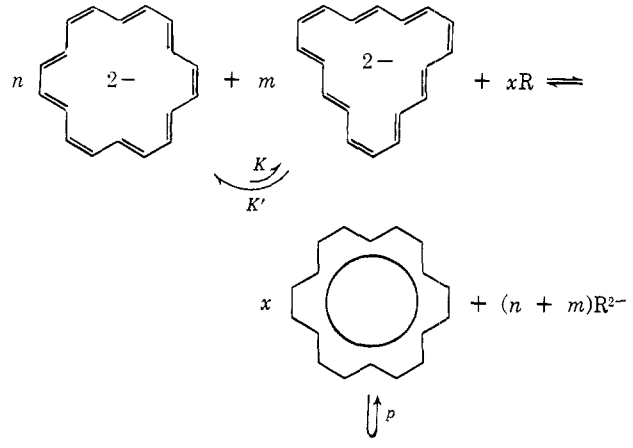

with (a) n/m = 70/30 (the observed proportion of [I]/[II]); (b) $(n + m)/x$ = 10–20 (since the neutral molecule **1** would be detected in the ^{1}H-nmr spectrum if present to the extent of 5–10%); and (c) K and K' indicate the conformational interconversion of I to II; p indicates the conformational mobility in the neutral molecule **1**.[6] It should be pointed out that, upon electron exchange, I would be converted into **1** and II into **2**, which then would transform into **1** (**2** is the postulated intermediate along the kinetic path of the conformational mobility of [18]annulene (**1**)[6]). The exchange diagram here is more complex than the one above (Figure 6). However, it reduces to it if, as is certainly the case, the electron-exchange processes are much faster (even though they are bimolecular) than the conformational mobility processes K amd K' (*i.e.*, V and V', interpreted now as being the rates of the processes involving electron exchange, are taken to be much larger than K and K').

(3) The third possibility that would allow a qualitative understanding of the temperature-dependent ^{1}H-nmr spectrum is the following: the two species are π-bond delocalized in their ground state and interconvert into each other by conformational mobility.

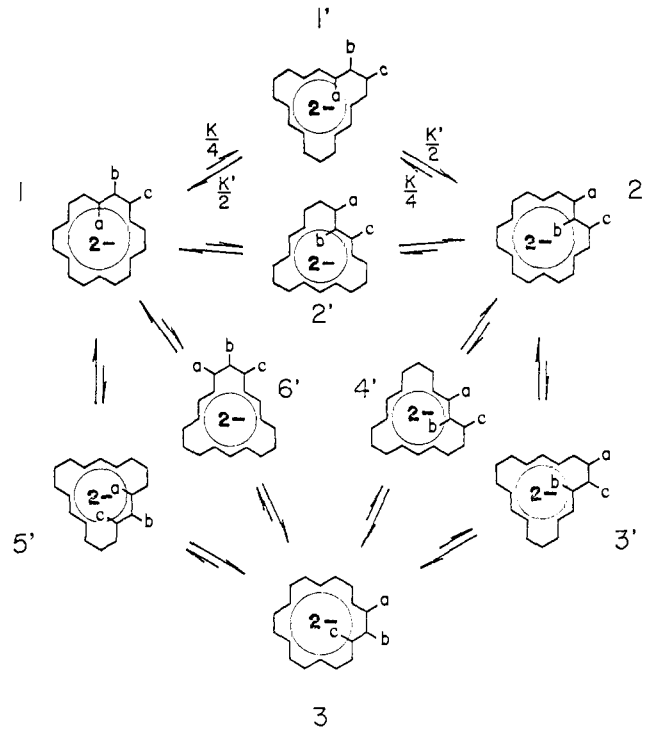

Figure 7. Exchange mechanism postulated to explain the magnetic equivalence of all the protons of the [18]annulene dianion above *ca.* −65° at 60 MHz. Ground-state structures with delocalized π bonds (III and IV, hypothesis 3) are considered.

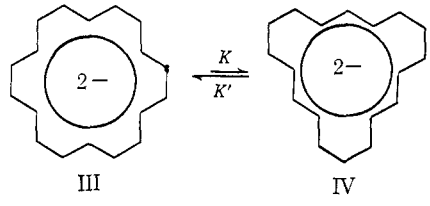

Three structures of type III and six of type IV are involved here, as indicated in Figure 7. The exchange diagram is simply the one given in Figure 8 (structure III has only two different magnetic sites and structure IV has four[19]). The conformational mobility in such structures would lead to complete exchange as indicated by the diagram. Note that this exchange diagram is, in fact, equivalent to the one given in Figure 6 (hypothesis 1) if, in the latter, $V = V' = \infty$.

Each of these three hypotheses has been tested by line-shape calculations using the stochastic exchange matrix method of Anderson–Kubo–Sack.[20] The expression for the line shape used is

$$I(\nu) = \mathrm{Re}\,(\mathbf{W}[2\pi i\mathbf{N} + \pi\Delta - \mathbf{A}]^{-1}\mathbf{U})$$

where **W** is the population line vector; its elements express how the different magnetic sites are occupied ($\Sigma_i w_i = 1$); **N** is a diagonal matrix, the elements of which are of the form $(\nu - \nu_i)$, ν being the frequency at which the intensity $I(\nu)$ is calculated and ν_i the frequency characteristic of the site i; Δ is a diagonal matrix; its elements are the line widths $\Delta\nu_i$ of the reso-

(19) Structures III and IV, planar with π bonds delocalized, could explain the spectrum observed at −110°. However, the paramagnetic shifts expected here would probably be much greater than those observed (see above in text).

(20) P. W. Anderson, *J. Phys. Soc. Jap.*, **9**, 316 (1954); R. Kubo, *ibid.*, **9**, 935 (1954); R. Kubo and K. Tomita, *ibid.*, **9**, 888 (1954); R. A. Sack, *Mol. Phys.*, 1, 163 (1958).

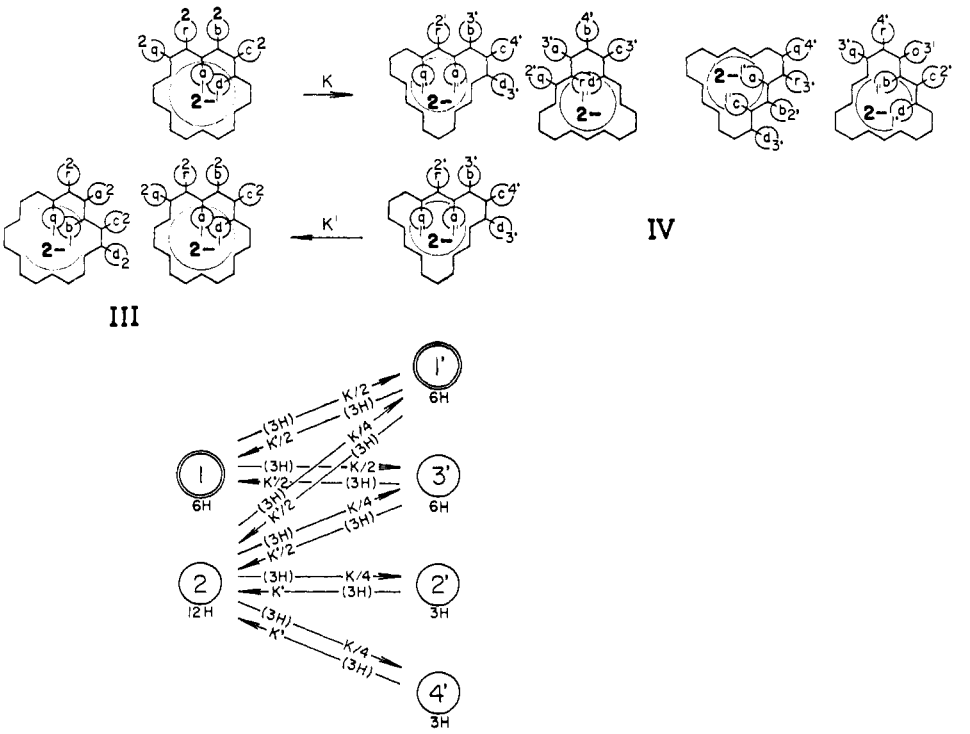

[18]annulene dianion

Exchange diagram

Hypothesis 3

Figure 8. Exchange diagram for the [18]annulene dianion. III and IV represent structures with delocalized π bonds which interconvert by a conformational process (K and K') (hypothesis 3).

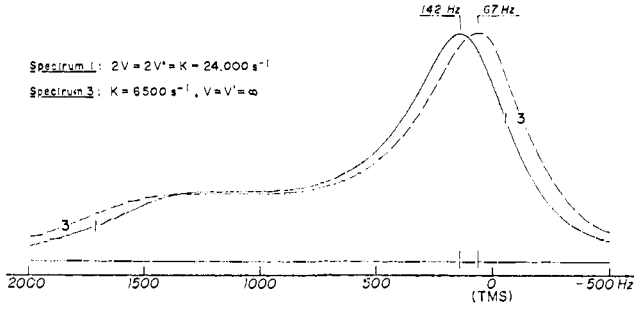

Figure 9. ^{1}H-nmr line shape at the second coalescence calculated according to hypothesis 1 (curve 1; $2V = 2V' = K = 24{,}000$ sec^{-1}) and according to hypothesis 3 (curve 3; $K = 6{,}500$ sec^{-1}, $K' = 15{,}160$ sec^{-1}).

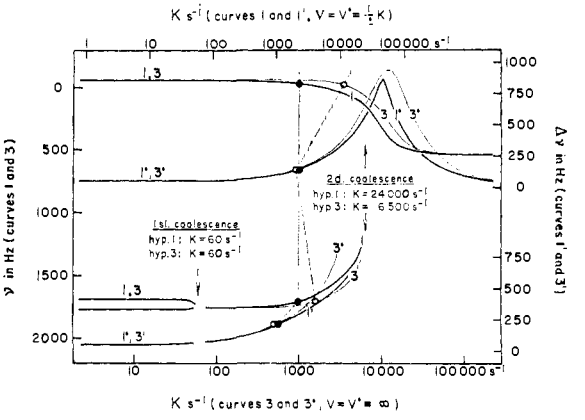

Figure 10. Position of the maxima (in Hz) and widths (in Hz) of the different signals appearing in the spectra computed according to hypothesis 1 (curves 1 and 1′) and to hypothesis 3 (curves 3 and 3′) as a function of the rate parameter K.

Table II

Hypothesis	Relationship between the kinetic parameters	Coalescence 1; K, sec^{-1}	Coalescence 2; K, sec^{-1}
1	$V = V' = K/2, K' = 70K/30$	60	24,000
	$V = 0, V' = K/2, K' = 70K/30$	60	24,000
	$V = V' = K/20, K' = 70K/30$		190,000
1 (also 2)	$V = V' = 10K/20, K' = 70K/30$		7,500
2 (also 1)	$V = V' = 1000K/2, K' = 70K/30$	60	6,600
3	$K = 30K'/70 (V = V' = \infty)$	60	6,500

nance signals in absence of exchange; **A** is the stochastic exchange matrix; its off-diagonal elements a_{ij} are the exchange probability densities for a proton to leave site i for site j; the diagonal elements are obtained as $a_{ii} = -\Sigma_j a_{ij}$; **U** is a column vector, the elements of which are all equal to 1.

In the case of hypotheses 1 and 2, the total number of sites is nine. They are identified as sites 1, 2, 3, 1′, ...6′; the elements of the vectors and of the matrices are indexed accordingly. The population vector **W** is: **W** = (7/30, 7/30, 7/30, 1.5/30, 1.5/30, 1.5/30, 1.5/30, 1.5/30, 1.5/30). The elements of the 9 × 9 matrices **N** and Δ are immediately obtained, taking (from the spectrum at −110°): $\nu_1 = 1770$ Hz, $\Delta\nu_1 = 35$ Hz;[21]

(21) These line widths were chosen for computation convenience. They correspond to the line widths observed in the spectrum at −110°.

$\nu_2 = \nu_3 = -65$ Hz, $\Delta\nu_2 = \Delta\nu_3 = 50$ Hz;[21] $\nu_{1'} = \nu_{3'} = 1685$ Hz, $\Delta\nu_{1'} = \Delta\nu_{3'} = 35$ Hz;[21] $\nu_{2'} = \nu_{4'} = \nu_{5'} = \nu_{6'} = -65$ Hz, $\Delta\nu_{2'} = \ldots = \Delta\nu_{6'} = 50$ Hz.[21]

The stochastic matrix **A** is written as (noting that $K' = 70K/30$)

Matrix A

A =	1	2	3	1′	2′	3′	4′	5′	6′
1	$-K$			$K/2$			$K/2$		
2		$-K - V$	V		$K/2$	$K/2$			
3		V	$-K - V$					$K/2$	$K/2$
1′	K'			$-K' - V'$		V'			
2′		K'			$-K'$				
3′		K'		V'		$-K' - V'$			
4′	K'						$-K' - V'$		V'
5′			K'					$-K'$	
6′			K'				V'		$-K' - V'$

In the case of hypothesis 3, the total number of sites is six. They are identified as sites 1, 2, 1′, 2′, 3′, 4′; the elements of the vectors and of the matrices are indexed accordingly. The population vector **W** is: **W** = (7/30, 14/30, 3/30, 1.5/30, 3/30, 1.5/30). The elements of the 6×6 matrices **N** and Δ are obtained taking: $\nu_1 = 1770$ Hz, $\Delta\nu_1 = 35$ Hz;[21] $\nu_2 = -65$ Hz, $\Delta\nu_2 = 50$ Hz;[21] $\nu_{1'} = 1685$ Hz, $\Delta\nu_{1'} = 35$ Hz;[21] $\nu_{2'} = \nu_{3'} = \nu_{4'} = -65$ Hz, $\Delta\nu_{2'} = \Delta\nu_{3'} = \Delta\nu_{4'} = 50$ Hz.[21]

The stochastic exchange matrix is ($K' = 70K/30$)

A =	1	2	1′	2′	3′	4′
1	$-K$		$K/2$		$K/2$	
2		$-K$	$K/2$		$K/2$	
1′	$K'/2$	$K'/2$	$-K'$			
2′		K'		$-K'$		
3′	$K'/2$	$K'/2$			$-K'$	
4′		K'				$-K'$

Table II summarizes the different relationships between the kinetic parameters that were chosen for the line-shape calculations. For each case investigated, the rate K (the reference rate is here K) was varied between 10 and 10^6 sec^{-1} in order to obtain all the line-shape patterns (up to the fast exchange limit) and to find the rates for which the coalescence of the signals of the inner protons (τ −19.5 and −18.1) (lower temperature or first coalescence) and the coalescence of all the signals into one single line (higher temperature or second coalescence) occur. The values of K for these coalescences are also given in the table. Very similar line shapes are obtained from computations based on the three hypotheses (*i.e.*, carried out with different relationships between the kinetic parameters). This is illustrated by the two spectra reproduced in Figure 9. They both correspond to the second coalescence and were computed with the following parameters: spectrum 1 (hypothesis 1), $V = V' = K/2 = 12{,}000$ sec^{-1} and $K' = 56{,}000$ sec^{-1}; spectrum 3 (hypothesis 3), $K = 6500$ sec^{-1} and $K' = 15{,}160$ sec^{-1}. These two spectra differ only slightly in shape: the maxima are not exactly at the same frequency (spectrum 1, $\nu_{max} = 142$ Hz; spectrum 3, $\nu_{max} = 67$ Hz) and the intensities in the high-frequency (low field) region are slightly different when the two spectra are normalized for the same maximum intensity.

Such minor differences in the computed line shapes are exploitable for solving the mechanistic problem, if they can be compared with corresponding features in the experimental spectra. The signal-to-noise ratio of the experimental spectra being very poor, we had to find the most apparent features which would allow us to test the different hypotheses. In Figure 10, we have compared the line-shape evolutions as computed according to hypothesis 1 ($V = V' = K/2$, $K' = 30K/70$) and to hypothesis 3 ($K = 30K'/70$, $V = V' = \infty$). The positions of the maxima of the different signals and their line widths are plotted against their corresponding value of K. The two sets of data are presented with the same scales for ν and $\Delta\nu$ (in Hz) but the two scales for the rate K have been adjusted so that the coalescence points coincide. This graph shows that, just below the second coalescence, the signals of the inner and outer protons are shifted toward each other to a greater extent for the same broadening in the case of hypothesis 1. Above the second coalescence, the exchange signal, taken at the same line width, has its maximum at approximately the same position for the two hypotheses.

Close inspection of the experimental spectra recorded between −85 and −65° led us to the conclusion that hypothesis 3 is not correct. The observed relationship between line widths and positions of the maxima of the signals is better explained by hypothesis 1 (see, for instance, the experimental data taken from the spectrum at −85° and reported in the graph).

Hypothesis 2 can be rejected on the following basis. The rates of electron exchange (equivalent to V and V') between the dianion and the neutral molecule should be a function of the concentration of these unreduced molecules. Consequently, the line shape observed at a given temperature should not be reproducible if further contact time between the solution and the potassium is allowed. This was tested at −80° and the line

Such an approximation does not invalidate the conclusions drawn from the comparison of the line shapes computed according to the different hypotheses.

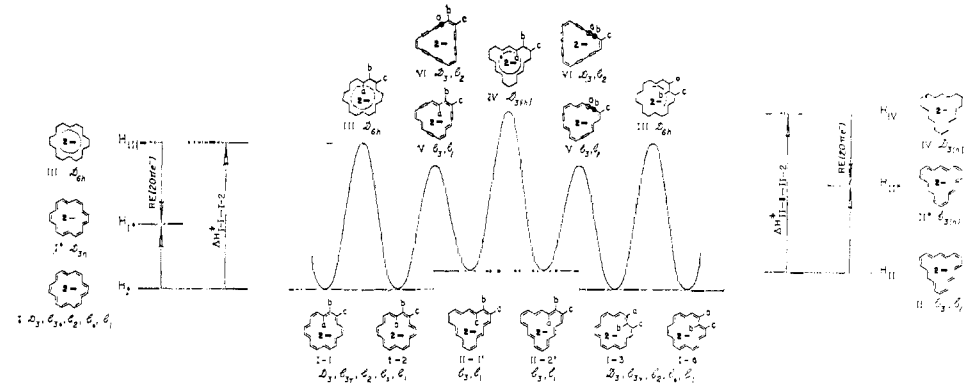

Figure 11. (Middle) Energy profile for a succession of the following processes (as implied by hypothesis 1): bond shift in I (V), conformation change I → II (K), bond shift in II (V'), conformation change II → I (K'), bond shift in I (V). (Left and right) Thermochemical evaluation of the resonance energy (RE) associated with 20 π electrons delocalized over 18 centers with geometries such as III (left) or IV (right).

shape was found to be independent of the various overall contact times (8–15 days at −80°).[22]

The analysis of the temperature-dependent ^{1}H-nmr spectra thus favors the structures I and II (with localized π bonds) proposed; I and II undergo fast π-bond shift (V and V') and interconvert one into each other by rotation around single bonds (K and K'). Although the signal-to-noise ratios of the experimental spectra were not good enough for quantitative line-shape fitting, we could, however, estimate the values of the kinetic parameters at −85, −65, and 0°. The results are reported in Table III. It should be pointed

Table III

Temp, °C	K, sec^{-1}	$V = V'$, sec^{-1}	K', sec^{-1}	$\Delta G^{\ddagger}$ (K), kcal mol^{-1}	$\Delta G^{\ddagger}$ (V, V'), kcal mol^{-1}
−85	2,200	1,100	5,133	8.0	8.2
−65	24,000	12,000	56,000	7.9	8.1
0	85,000	42,500	198,300	9.8	10.1
				⟨8.5⟩	⟨8.8⟩

out that these results were obtained assuming $V = V' = K/2$. However, it can be shown that the values of $\Delta G^{\ddagger}$ one would obtain taking $V = V' = 10K/2$ or $V = V' = K/20$ would not differ by more than 1 kcal mol^{-1} from those reported. The free energy of activation for all processes (K, V, and V') is thus: $\Delta G^{\ddagger} = 8.7 \pm 1.5$ kcal mol^{-1}. It is interesting to note that this value is very close to those measured for the conformational mobilities and the π-bond shift processes taking place in [16]-85- and [16]-91-annulene.[10,14]

Conclusions

A. Structure of the [18]Annulene Dianion and the π-Bond Situation. From the analysis of the ^{1}H-nmr spectrum (in absence of exchange, *i.e.*, at −110°) and of its temperature dependence, we conclude that the two species obtained by reduction of [18]annulene are two conformers of the dianion with 219 configuration (structures I and II). These species are most likely nonplanar and exhibit π-bond alternation; each species undergoes a fast π-bond shift process and interconverts into the other one by rotation around single bonds (conformational mobility).

B. Kinetic Pathway for the Dynamic Processes Observed in the [18]Annulene Dianion. The most likely pathway for both the conformational mobility (rates $K/2$ and K') and the π-bond shift processes in [18]annulene dianion is illustrated in Figure 11. The conformational mobility requires rotation around single bonds (six or more), thus leading to transition-state structures with double bonds perpendicular to the mean plane of the dianion (such as structures V and VI). These transition-state structures are analogous to those postulated for the conformational mobility in [18]-annulene itself (several structures of type V as well as of type VI with different symmetries are possible; see ref 6). The bond-shift processes in structures I and II imply a flattening of these structures with progressive π-bond delocalization; likely transition-state structures are III and IV, already discussed and rejected as ground-state structures. Structure III would be planar (D_{6h} symmetry); IV cannot be planar but would approach planarity closely enough for π-bond delocalization to occur (symmetry D_3 or C_2 depending on how the inner hydrogens interlock).

In Figure 11 the relative positions (in enthalpy) of the ground-state structures I and II and of the transition-state structures III, IV, V, or VI are arbitrarily given. Their correct relative positions could not be obtained, since this determination would require a quantitative line-shape analysis with fitting of the ^{1}H-nmr spectra over a wide temperature range with adjustment of four kinetic parameters ($K/2$, K', V, and V'), *i.e.*, a procedure which could not be carried out due to the poor signal-to-noise ratio of the spectra. We could show, however, that the activation free energy, and thus the activation enthalpy, for the bond-shift processes in I and II is of the order of 8.7 kcal mol^{-1} (see Table III).

C. Resonance Energy Associated with a Delocalized π-Bond System of 20 π Electrons and 18 sp^2 Carbon Atoms. If the kinetic pathway that we propose for the π-bond shift processes in I and II is correct, the activation energy allows us to evaluate the resonance energy (RE) associated with π bonds (20 π electrons) delocalized over 18 sp^2 carbon atoms, such as in structures III and IV. The thermochemical diagrams on both

(22) The concentrations, at the reduction equilibrium, of the neutral molecule and of the radical anion are expected to be negligible (and not to contribute to the exchange), since the reduction potential $K^- + e^- \rightleftharpoons K$ is over 1 V more negative than the second reduction wave of [18]annulene ($R \cdot^- + e^- \rightleftharpoons R^{2-}$).

sides of Figure 11 indicate how this estimation can be made. Each activation enthalpy $\Delta H^{\ddagger}_{\text{I-1}\rightarrow\text{I-2}}$ and $\Delta H^{\ddagger}_{\text{II-1}'\rightarrow\text{II-2}'}$ can formally be considered as the sum of two enthalpy differences, as indicated in the figure: $\Delta H^{\ddagger}_{\text{I-1}\rightarrow\text{I-2}} = H_{\text{III}} - H_{\text{I}} = (H_{\text{III}} - H_{\text{I}}^{*}) + (H_{\text{I}}^{*} - H_{\text{I}})$ and $\Delta H^{\ddagger}_{\text{II-1}'\rightarrow\text{II-2}'} = H_{\text{IV}} - H_{\text{II}} = (H_{\text{IV}} - H_{\text{II}}^{*}) + (H_{\text{II}}^{*} - H_{\text{II}})$. The first difference in each of these expressions is the resonance energy of III and IV, respectively, since I* and II* are hypothetical structures with π-bond localization (with normal single and double bonds) and with the same degree of planarity as III and IV. (III and I* are presumed to be planar; IV and II* are presumed to approach planarity as much as is compatible with nonbonding interactions between the inner hydrogens.) The second difference expresses how much energy is required to force the nonplanar ground-state structures I and II into planar or quasiplanar geometries (*i.e.*, into I* and II*, respectively). The energy difference $H_{\text{I}}^{*} - H_{\text{I}}$ was estimated to be of the order of 3 kcal mol^{-1} or less,[6] the planar Kekulé structure I* thus being higher in energy than the nonplanar ground-state structure I in which the nonbonding interactions between the inner protons and the strain energy are considered to be minimized. The difference $H_{\text{II}}^{*} - H_{\text{II}}$ could not be estimated since II* (or IV) as well as II have unknown geometries. Most likely II* and IV (and thus II) have very similar geometries and the difference $H_{\text{II}}^{*} - H_{\text{II}}$ is therefore probably close to zero.

Thus, we can conclude that the resonance energy associated with 20 π electrons delocalized over π-bond systems of geometries such as III (planar, 18 sp^2 carbon atoms) or IV (quasiplanar, 18 sp^2 carbon atoms) is negative and lies between -8.7 and -5 kcal mol^{-1}.

$$\text{RE}\,(20\ \pi\ \text{e}^{-}/18\ \text{sp}^2\ \text{C}) = -5\ \text{to}\ -8.7\ \text{kcal mol}^{-1}$$

It is interesting to note that resonance energy values of -2.8 kcal mol^{-1} (P. P. P. method) and of -7.2 kcal mol^{-1} (S. P. O. method) were found by semiempirical SCF calculations for the planar [20]annulene (of configuration 439) with delocalized π bonds.[11]

Acknowledgments. We acknowledge, with gratitude, the support of the Schweizerische National Fonds and of the Swiss Chemical Industries (Ciba-Geigy, Lonza, and Hoffmann-La Roche). One of us (E. P. W.) is indebted to the National Research Council of Canada for a Postdoctoral Fellowship (1968–1969). We thank also Dr. J.-M. Gilles for the line-shape calculations.

Conformational Effects of Alkyl Groups on the $\pi \rightarrow \pi^*$ Transitions of α-Enones

Alain Bienvenüe

Contribution from Laboratoire de Chimie Organique Physique de l'Université Paris VII, associé au C.N.R.S., 75005 Paris, France. *Received February 21, 1973*

Abstract: The ir and uv spectra ($\pi \rightarrow \pi^*$ transition) of 18 cis and trans α-enones, RCOCH=CHMe, have been studied (R = Me, Et, Pr, *i*-Bu, *i*-Pr, *t*-Bu, neoPe, –CH(Me)-*t*-Bu, and –CMe$_2$-*t*-Bu). The molar fractions of all the conformers are calculated from the ir spectra of the enones, assuming that the specific intensities of all the $\nu_{C=O}$ bands are constants. For trans enones the s-trans $\rightleftharpoons$ s-cis equilibrium is displaced toward the s-cis form when R varies in the order Me, Et, Pr, *i*-Bu, neoPe, –CHMe-*t*-Bu, *i*-Pr, *t*-Bu, or –CMe$_2$-*t*-Bu, whereas the cis enones are exclusively s-cis. For R = neoPe, –CH(Me)-*t*-Bu, and –CMe$_2$-*t*-Bu in addition, it has been possible to calculate the contribution of the gauche conformation of R (for enones in the s-cis or in the s-trans forms) where the *t*-Bu substituent does not eclipse the carbonyl. In this conformation one of the Me groups of *t*-Bu is close to the C=C bond and gives rise to $\nu_{C=C}$ shifts. In the electronic spectrum, a constant $\nu_{\pi\rightarrow\pi^*}$ wave number is found to be associated with each possible set of enone (s-cis or s-trans) and R (eclipsed or gauche) conformations, regardless of the nature of R and the configuration of the enone. When an enone is a mixture of conformations, a linear combination of these $\nu_{\pi\rightarrow\pi^*}$ (using the previously calculated conformer fractions) is shown to give a ν_{max} in very good agreement with experimental results. The ν_{max} for the s-cis conformation is found to be 2400 cm^{-1} lower than that of the s-trans conformation (47,500 cm^{-1}) and an additional bathochromic shift of 800 cm^{-1} is observed when a Me group is close to the C=C bond.

Woodward's rules,[1] which relate the position of the $\pi \rightarrow \pi^*$ transition to the number of alkyl substituents in the R_α, $R_{\beta c}$, or $R_{\beta t}$ positions of enones, are well known, and their analytical utility is beyond question. It is curious, however, to note that there have been few attempts to explain them theoretically. The following are two typical approaches: that of Allinger, *et al.*,[2] who apply a modified Pariser–Parr treatment to cyclic enones in conformations approximating to s-cis or s-trans; that of Luft and Basso[3] who calculate by a *w*, *w'*, *w''* SCF method the effect of progressively substituting hydrogen atoms by methyl groups in the skeleton MeCOC=C. The two calculations lead to results no closer to experimental values (about 2–5 nm) than Woodward's empirical rules. It is likely that these differences are caused in part by the failure to take into account the variations of the bond angles in cyclic systems or the conformational modifications imposed by substitution in labile system.

(1) R. B. Woodward, *J. Amer. Chem. Soc.*, **63**, 1123 (1941).
(2) N. L. Allinger, T. W. Stuart, and J. C. Tai, *ibid.*, **90**, 2809 (1968).
(3) R. Luft and J. Basso, *C. R. Acad. Sci., Ser. C*, **265**, 980 (1967).